

INVERSE PROBLEM FOR AXISYMMETRICAL PARABOLOIDAL GAS TURBINE STAGE

ROMUALD PUZYREWSKI

KRYSTYNA NAMIEŚNIK

Institute of Fluid-Flow Machinery of the Polish Academy of Sciences

e-mail: knam@imppan.imp.pg.gda.pl

The paper presents a solution to the inverse problem for a gas turbine stage within the frame of axisymmetrical stationary flow model. The shapes of axisymmetrical stream surface are assumed to be paraboloidal and flow is isentropic. The solution yields the curvatures of blade channels and the distribution of parameters in the entire flow field.

Key words: turbine, turbomachinery, subsonic flow, flow modeling

1. Introduction

Although the axisymmetrical models have been already commonly used in engineering applications for turbomachine stages calculations (cf Wennstrom (1974), Bütikofer et al. (1989)), the inverse approach seems to be rather new in the design problems. The inverse approach is a discipline which is growing very rapidly in the field of engineering. This approach can support the design procedures very efficiently if the problems are formulated in the way which allows one to find an effective solution.

In the presented example the inverse approach is based on the assumptions that axisymmetrical stream surfaces are known in the form of paraboloidal shapes as it is shown in Fig.1. One can build the coordinate system based on such paraboloidal surfaces using them as the coordinate surfaces. The family of planes perpendicular to the axis of the stage and the family of meridional planes which contain the axis can be treated as the second and the third coordinate surfaces, respectively. Such a coordinate system is described by Puzyrewski and Namieśnik (1993). For the nozzle blade flow the solution in

such a coordinate system was presented by Puzyrewski and Namieśnik (1995). The paper presents the solution for the whole stage; i.e., nozzle, gap and rotor domains fitted into such a coordinate system. Unlike a similar solution for conical coordinate system as it was formulated by Puzyrewski and Pozorski (1993) the present example includes the curvatures of stream lines in a meridional cross section. Moreover, the inclination of the blading domain interfaces in axial directions as it is shown in Fig.2 causes an additional complication in the algorithm of rotor domain.

2. Basic assumptions

The assumptions on the model of the flow is formulated can be separated into groups. The main assumptions are: the stationary and axisymmetrical flow model.

The assumption of stationary flow excludes the main mechanism of the energy subtraction from the flow. In the real turbomachinery stage the main mechanism of the energy subtraction follows from $\partial p/\partial t = 0$. If the condition $\partial/\partial t = 0$ holds, then one has to introduce energy subtraction from the flow, in accordance with the Euler formula

$$-a = \left(U_r U_{x(2)} \right)_0 - \left(U_r U_{x(2)} \right)_1 \quad (2.1)$$

where

$$\begin{aligned} U_{x(2)} &- \text{circumferencial velocity of the flow} \\ U_r &- \text{rotor circumferencial velocity} \end{aligned}$$

and the subscripts 0 and 1 denote the corresponding positions along the axis of the stage. For the nozzle flow and for the gap flow $U_r \equiv 0$, which simply means conservation of total energy. The energy is subtracted at the rotor inlet, where $U_r \neq 0$. This is rather a rough model due to the discontinuity in energy transfer from the flow at the rotor inlet of the stage.

The second assumption of axisymmetry makes the cascades "invisible". On the assumption that all derivatives in the circumferencial direction vanish, the governing equations become more simple. As a consequence, the existence of real cascade has to be represented in the mass conservation, momentum, energy and entropy equations, respectively in the way which reflect the existence of blading.

In the mass conservation equation the blockage factor $\tau(x^{(1)}, x^{(3)})$ corresponds to the fraction of the space occupied by blading, i.e. not available for the flow.

In the momentum conservation equation the existence of the blading can be represented by the reaction force continuously distributed in region of blading. In a general case the reaction force has three components. Here, for the coordinate system based on parabolic surfaces the reaction force will be presented only by components in the plane tangential to the parabolic surfaces, which means

$$F_{x(1)} \equiv 0 \quad F_{x(2)} \neq 0 \quad F_{x(3)} \neq 0 \quad (2.2)$$

Thus the model is simplified because it removes one unknown $F_{x(1)} \equiv 0$.

In the energy equation the subtraction of energy appears only in the rotor domain by formula (2.1) whereas in the nozzle and gap domains the total energy is conserved as noted above.

In the entropy balance equation the dissipation losses can be modelled assuming a certain distribution of entropy in the field of nozzle, gap and rotor. Then one can use the formula

$$\frac{p}{\rho^\kappa} = \frac{p_0}{\rho_0^\kappa} \exp\left[\frac{\kappa-1}{R}(S-S_0)\right] \quad (2.3)$$

where S has to be chosen as a function of position in the flow domain, presuming a certain level of losses. For the isentropic model one can assume $S = S_0$ and formula (2.3) reduces to the isentropic one

$$\frac{p}{\rho^\kappa} = \frac{p_0}{\rho_0^\kappa} \quad (2.4)$$

3. Geometry of the stage

The stage considered here has the form of the following parabolic stream surfaces

$$r = r_w + \frac{hz}{z_0} \left(2 - \frac{z}{z_0}\right) \quad (3.1)$$

where r_w and z_0 are the parameters shown in the Fig.1.

The parameter h identifies the parabola and will be treated as the first coordinate

$$x^{(1)} = h$$

Along the circumference the angle φ will be chosen as the second coordinate

$$x^{(2)} = \varphi$$

and the third coordinate is

$$x^{(3)} = z$$

In the paraboloidal coordinate system formula (3.1) can be rewritten as

$$r = f(x^{(1)}, x^{(3)}) = r_w + \frac{x^{(1)}x^{(3)}}{z_0} \left(2 - \frac{x^{(3)}}{z_0}\right) \tag{3.2}$$

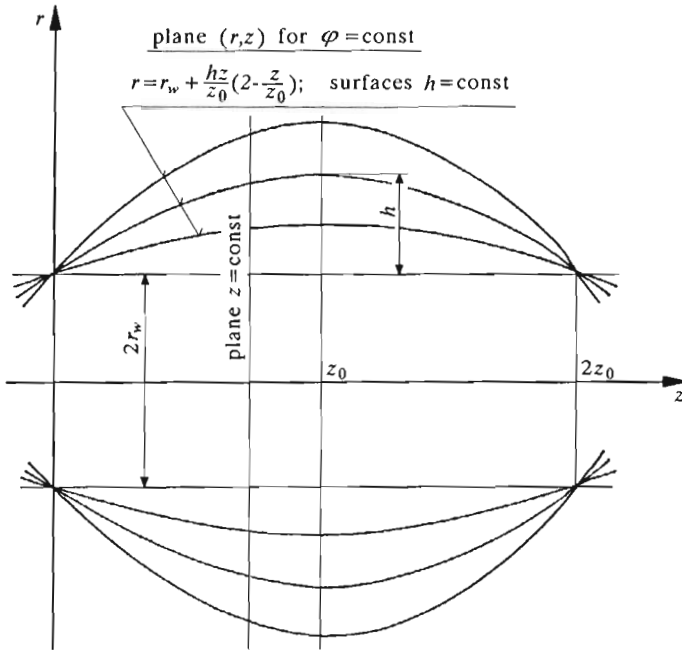


Fig. 1.

The system $x^{(1)}, x^{(2)}, x^{(3)}$ is non-orthogonal in pairs $(x^{(1)}, x^{(2)})$ and $(x^{(1)}, x^{(3)})$ and orthogonal in the pair $(x^{(2)}, x^{(3)})$.

The axial borders of the nozzle are at the inlet

$$z_{00} = \text{const}$$

and at the outlet

$$z_1 = z_{10} + \tan \phi_1 (r - r_w)$$

while for the rotor at the inlet

$$z_2 = z_{20} + \tan \phi_2 (r - r_w)$$

and at the outlet

$$z_3 = z_0 + \tan \phi_3(r - r_3)$$

where ϕ_1, ϕ_2, ϕ_3 are the inclinations of conical domain interfaces in the (r, z) plane as it can be seen in Fig.2.

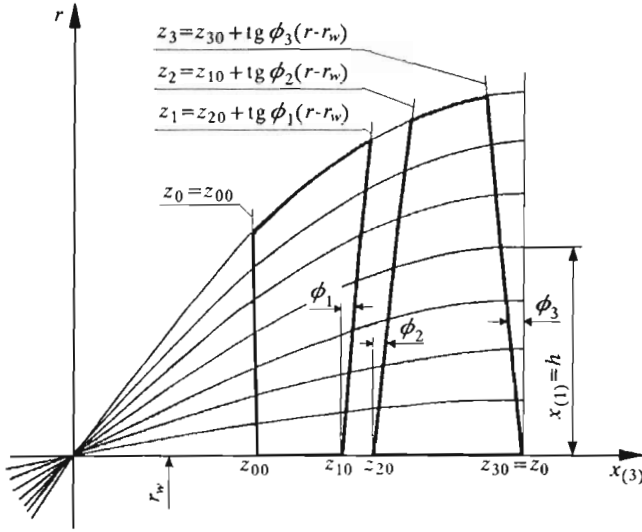


Fig. 2.

4. Governing equations

In non-orthogonal system $x^{(1)}, x^{(2)}, x^{(3)}$ the set of governing equations has the form presented by Puzyrewski and Namieśnik (1993), (1995).

With the help of relation (3.2) one can derive the mass conservation equation

$$\rho \frac{\left[r_w + \frac{x^{(1)}x^{(3)}}{z_0} \left(2 - \frac{x^{(3)}}{z_0} \right) \right] \frac{x^{(3)}}{z_0} \left(2 - \frac{x^{(3)}}{z_0} \right)}{\sqrt{1 + \left[\frac{2x^{(1)}}{z_0} \left(1 - \frac{x^{(3)}}{z_0} \right) \right]^2}} U_{x^{(3)}} \left(1 - \tau(x^{(1)}, x^{(3)}) \right) = m(x^{(3)}) \tag{4.1}$$

Momentum conservation equation in the $x^{(1)}$ direction

$$\begin{aligned} & \frac{\rho U_{x^{(2)}}^2}{r_w + \frac{x^{(1)}x^{(3)}}{z_0} \left(2 - \frac{x^{(3)}}{z_0}\right)} - \frac{\rho U_{x^{(3)}}^2 \frac{2x^{(1)}}{z_0^2}}{1 + \left[\frac{2x^{(1)}}{z_0} \left(1 - \frac{x^{(3)}}{z_0}\right)\right]^2} = \\ & = - \frac{1 + \left[\frac{2x^{(1)}}{z_0} \left(1 - \frac{x^{(3)}}{z_0}\right)\right]^2}{\frac{x^{(3)}}{z_0} \left(2 - \frac{x^{(3)}}{z_0}\right)} \frac{\partial p}{\partial x^{(1)}} + \frac{2x^{(1)}}{z_0} \left(1 - \frac{x^{(3)}}{z_0}\right) \frac{\partial p}{\partial x^{(3)}} \end{aligned} \quad (4.2)$$

in the $x^{(2)}$ direction

$$\frac{\rho U_{x^{(3)}}}{\sqrt{1 + \left[\frac{2x^{(1)}}{z_0} \left(1 - \frac{x^{(3)}}{z_0}\right)\right]^2}} \left[\frac{\partial U_{x^{(3)}}}{\partial x^{(3)}} + \frac{2x^{(1)}}{z_0} \left(1 - \frac{x^{(3)}}{z_0}\right) U_{x^{(2)}} \right] = \rho F_{x^{(2)}} \quad (4.3)$$

in the $x^{(3)}$ direction

$$\begin{aligned} & \frac{\rho U_{x^{(3)}}}{\sqrt{1 + \left[\frac{2x^{(1)}}{z_0} \left(1 - \frac{x^{(3)}}{z_0}\right)\right]^2}} \left[\frac{\partial U_{x^{(3)}}}{\partial x^{(3)}} + \frac{4x^{(1)^2}}{z_0^3} \left(1 - \frac{x^{(3)}}{z_0}\right) U_{x^{(3)}} \right] = \\ & = \rho F_{x^{(3)}} + \sqrt{1 + \left[\frac{2x^{(1)}}{z_0} \left(1 - \frac{x^{(3)}}{z_0}\right)\right]^2} \left[\frac{2x^{(1)}}{z_0} \left(1 - \frac{x^{(3)}}{z_0}\right) \frac{\partial p}{\partial x^{(1)}} - \frac{\partial p}{\partial x^{(3)}} \right] \end{aligned} \quad (4.4)$$

The energy conservation equation

$$\frac{1}{2} \left(U_{x^{(2)}}^2 + U_{x^{(3)}}^2 \right) + \frac{\kappa}{\kappa - 1} \frac{p}{\rho} - U_{x^{(2)}} U_r = h \left(x^{(1)} \right) \quad (4.5)$$

The isentropic condition

$$\frac{p}{\rho^\kappa} = c \left(x^{(1)} \right) \quad (4.6)$$

where

$$U_r = \frac{\pi r}{30} n \quad (4.7)$$

is the circumferential velocity of rotor for n in rpm.

The above set of equations is closed with respect to: ρ , $U_{x^{(2)}}$, $U_{x^{(3)}}$, $F_{x^{(2)}}$, $F_{x^{(3)}}$, p .

5. Method of solution

The method of solution was described by Puzyrewski and Namieśnik (1993), (1995). It is based on the fact that the solution of above equations can be reduced to the hyperbolic one

$$\begin{aligned}
 & -\frac{1 + \left[\frac{2x^{(1)}}{z_0} \left(1 - \frac{x^{(3)}}{z_0} \right) \right]^2}{\frac{x^{(3)}}{z_0} \left(2 - \frac{x^{(3)}}{z_0} \right)} \frac{\partial p}{\partial x^{(1)}} - \frac{2x^{(1)}}{z_0} \left(1 - \frac{x^{(3)}}{z_0} \right) \frac{\partial p}{\partial x^{(3)}} + \\
 & + O \frac{\partial U_{x^{(2)}}}{\partial x^{(1)}} + O \frac{\partial U_{x^{(2)}}}{\partial x^{(3)}} = R_1(x^{(1)}, x^{(3)}) \\
 & O \frac{\partial p}{\partial x^{(1)}} + \frac{\kappa}{\kappa - 1} \frac{\partial p}{\partial x^{(3)}} + O \frac{\partial U_{x^{(2)}}}{\partial x^{(1)}} + \rho U_{x^{(2)}} \left(1 - \frac{U_r}{U_{x^{(2)}}} \right) \frac{\partial U_{x^{(2)}}}{\partial x^{(3)}} = \\
 & = R_2(x^{(1)}, x^{(3)})
 \end{aligned} \tag{5.1}$$

$$\begin{aligned}
 dx^{(1)} \frac{\partial p}{\partial x^{(1)}} + dx^{(3)} \frac{\partial p}{\partial x^{(3)}} + O \frac{\partial U_{x^{(2)}}}{\partial x^{(1)}} + O \frac{\partial U_{x^{(2)}}}{\partial x^{(3)}} & = dp \\
 O \frac{\partial p}{\partial x^{(1)}} + O \frac{\partial p}{\partial x^{(3)}} + dx^{(1)} \frac{\partial U_{x^{(2)}}}{\partial x^{(1)}} + dx^{(3)} \frac{\partial U_{x^{(2)}}}{\partial x^{(3)}} & = dU_{x^{(2)}}
 \end{aligned}$$

where R_1 and R_2 are the right-hand side functions.

The set of above equations has the main determinant of the coefficient matrix equal to

$$W_0 = \rho U_{x^{(2)}} \left(1 - \frac{U_r}{U_{x^{(2)}}} \right). \tag{5.2}$$

$$\cdot \left[\frac{2x^{(1)}}{z_0} \left(1 - \frac{x^{(3)}}{z_0} \right) dx^{(1)} + \frac{1 + \left[\frac{2x^{(1)}}{z_0} \left(1 - \frac{x^{(3)}}{z_0} \right) \right]^2}{\frac{x^{(3)}}{z_0} \left(2 - \frac{x^{(3)}}{z_0} \right)} dx^{(3)} \right] dx^{(1)}$$

The condition $W_0 = 0$ defines two family of characteristics.

The first family is

$$x^{(1)} = \text{const} \tag{5.3}$$

The second family is

$$x^{(1)} - \frac{z_0^3}{x^{(3)}(2z_0 - x^{(3)})}. \tag{5.4}$$

$$\cdot \sqrt{\frac{1}{2} \left[\left(\frac{z'}{z_0} \right)^2 - \left(\frac{x^{(3)}}{z_0} \right)^2 \right] - \left(\frac{z'}{z_0} - \frac{x^{(3)}}{z_0} \right) - \ln \frac{z_0 - z'}{z_0 - x^{(3)}}} = \text{const}$$

where $z' = x^{(3)}$ at $x^{(1)} = 0$.

Along the characteristics (5.4) the equation

$$\frac{dp}{dx^{(1)}} = \frac{\rho U_{x^{(2)}}^2 \frac{2x^{(3)}}{z_0} \left(2 - \frac{x^{(3)}}{z_0}\right)}{r_w + \frac{x^{(1)}x^{(3)}}{z_0} \left(2 - \frac{x^{(3)}}{z_0}\right) 1 + \left[\frac{2x^{(1)}}{z_0} \left(1 - \frac{x^{(3)}}{z_0}\right)\right]^2} + \tag{5.5}$$

$$+ \frac{\rho U_{x^{(3)}}^2 \frac{2x^{(1)}}{z_0^2} \frac{x^{(3)}}{z_0} \left(2 - \frac{x^{(3)}}{z_0}\right)}{\left\{1 + \left[\frac{2x^{(1)}}{z_0} \left(1 - \frac{x^{(3)}}{z_0}\right)\right]^2\right\}^2}$$

has to be satisfied. The boundary conditions have to be imposed at the borders where the characteristics (5.4) starts as shown in Fig.3. The domain of the nozzle $A_0B_0B_1A_1$ is covered by the family of characteristics (5.3) starting at the inlet of the nozzle A_0B_0 and by the characteristics of the second family starting either from the inlet $A'_0A''_0A'''_0\dots$ etc or from the upper border $B'_0B''_0B'''_0\dots$ etc. The arrow shows the direction of integration.

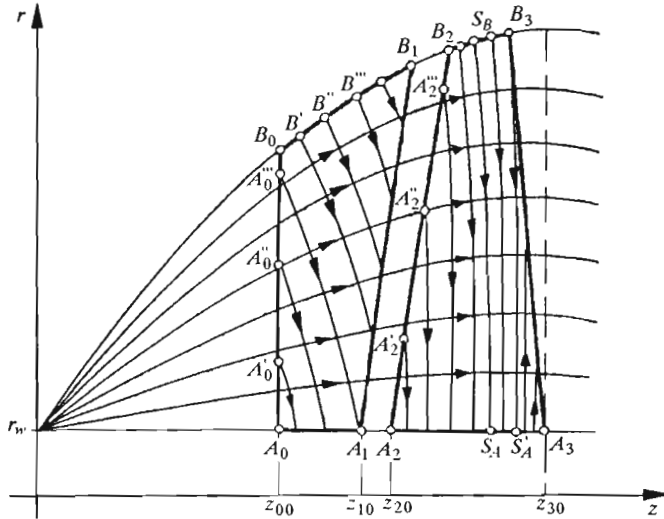


Fig. 3.

The domain of the gap $A_1B_1B_2A_2$ is easy to integrate explicitly because the reaction force components $F_{x^{(2)}} = F_{x^{(3)}} = 0$ vanish.

The domain of the rotor $A_2B_2B_3A_3$ is divided into three subdomains where the integration is handled differently. As it follows from the determinant (5.2) the points at which $U_{x^{(2)}} = U_r$ are singular. If this condition occurs at

the outer border of rotor B_2B_3 , at the point, say, S_B then the characteristics starting at this point may be regarded as a singular line, where $U_{x(2)} = U_r$. This cuts the subdomain $A_2B_2S_AS_B$ out of the rotor. Here $U_{x(2)}$ changes its value from those known from the solution in the gap region at the line A_2B_2 to the value of $U_{x(2)} = U_r$ at the singular line S_AS_B . If one assumes the function $U_{x(2)}(x^{(1)}, x^{(2)})$ which fulfills the boundary conditions along the lines A_2B_2 and S_AS_B , then Eq (5.5) for the pressure can be integrated and the blockage factor $\tau(x^{(1)}, x^{(3)})$ can be obtained. The blockage factor determines the relative thickness of profiles in the region.

For the second subdomain in the rotor S_A, S_B, B_3, S'_A , the characteristics which starts at the line S_BB_3 can be integrated on the assumption of blockage factor $\tau(x^{(1)}, x^{(3)})$. In contrast to the first subdomain, here $\tau(x^{(1)}, x^{(3)})$ is known and $U_{x(2)}$ is the resulting function.

At the point S'_A , one knows $U_{x(2)}$ from the integration along $B_3S'_A$. If one assumes the behavior of $U_{x(2)}$ along S'_AA_3 then the solution can be found in the third subdomain $S'_AB_3A_3$. Here the direction of integration is shown by the arrows. In this subdomain the blockage factor $\tau(x^{(1)}, x^{(3)})$ has to be given and has to account for the relative trailing edge thickness along the exit line A_3B_3 .

6. Numerical example

For the numerical example the gas turbine stage with the geometrical proportions shown in Fig.4 was taken. The inlet static parameters were

$$p_0 = 6 \text{ bars} \qquad T_0 = 1000 \text{ K}$$

For the mass flow rate

$$m = 12.6 \text{ kg/s}$$

the uniform axial component of velocity at the inlet to the nozzle was

$$U_0 = 47.8512 \text{ m/s}$$

At the upper border of the nozzle domain a linear distribution of $U_{x(2)}$ component was assumed up to 350 m/s. The velocity components at the points A_3 and B_3 were $U_{x(2)} = -100 \text{ m/s}$ and $U_{x(2)} = 0 \text{ m/s}$, respectively.

The gas constants were

$$R = 287 \text{ kJ/(kgK)} \qquad \kappa = 1.4$$

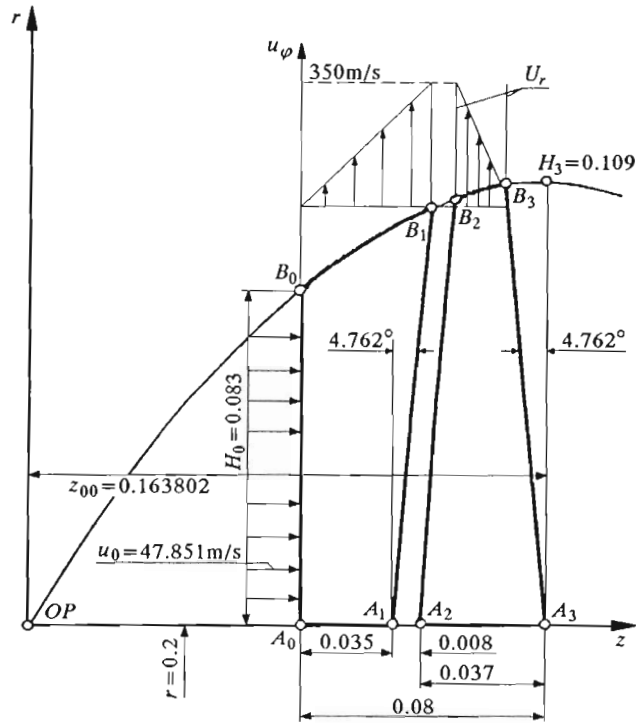


Fig. 4.

• Nozzle flow

The upper boundary condition set as linear velocity $U_{x(2)}$ led to the pressure distribution along the arc B_0B_1 . The blockage factor in form of the function

$$\tau(x^{(1)}, x^{(3)}) = \left(0.1 + 0.1 \frac{0.109 - x^{(1)}}{0.109}\right) \left(\frac{1 - \bar{x}^{(3)}}{0.5}\right)^2 \left(\frac{\bar{x}^{(3)}}{0.5}\right)^2$$

was introduced into the nozzle domain. Here $\bar{x}^{(3)}$ is the relative width of nozzle blading changing from 0 at the inlet to 1 at the outlet along the coordinate axis $x^{(3)}$.

The main aim of the calculations was to find the surfaces S_2 as it is shown in Fig.5 for radially positioned generatrix. The results of calculation are shown in Fig.6 in the form of S_2 surface. The distribution of parameters at the outlet enabled us to start with the calculations of the gap domain.

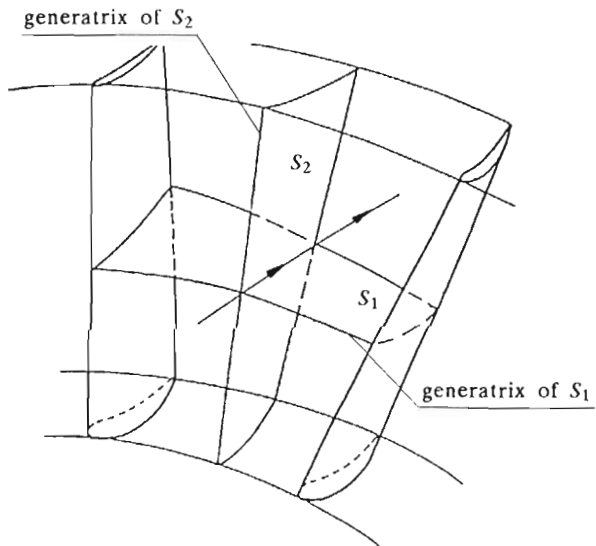


Fig. 5.

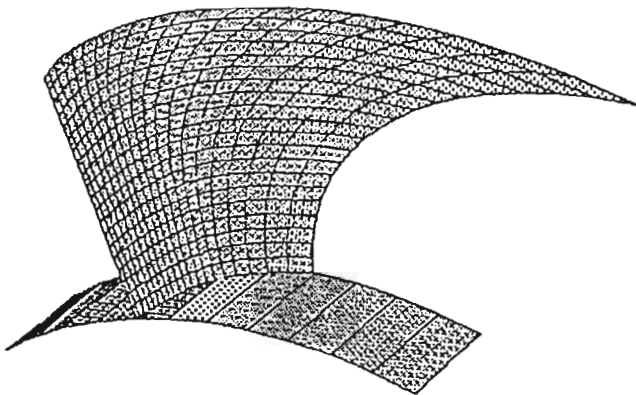


Fig. 6.

- Gap flow

The flow parameters within the gap can be found by the direct integration. The exit parameters at the gap were startig parameters for the rotor domain. The Fig.7 surface of type S_2 for the gap is shown in Fig.7.

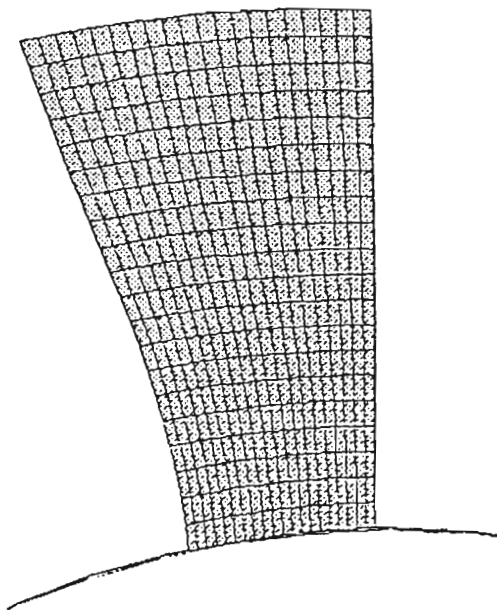


Fig. 7.

- Rotor flow

The first subdomain of the rotor (left to singular line) was covered by the linear change of $U_{x^{(2)}}$ velocity component from the value at rotor inlet to the value $U_{x^{(2)}} = U_r$ at the singular line where U_r results from $n = 8000$ rpm. In the second and third subdomains S_A, S_B, B_3, S'_A and $S'_A B_3 A_3$, respectively, the blockage factor was introduced in the form

$$(x^{(2)}, x^{(3)}) = \tau_3 \left[(\bar{x}^{(3)})^{0.1} + 0.1(1 - \bar{x}^{(3)})^{1.25} \right]$$

where τ_s is the blockage factor at the singular line and $\bar{x}^{(3)}$ is the relative width of the rotor blade startig with 1 at singular line and ending with 0 at the exit.

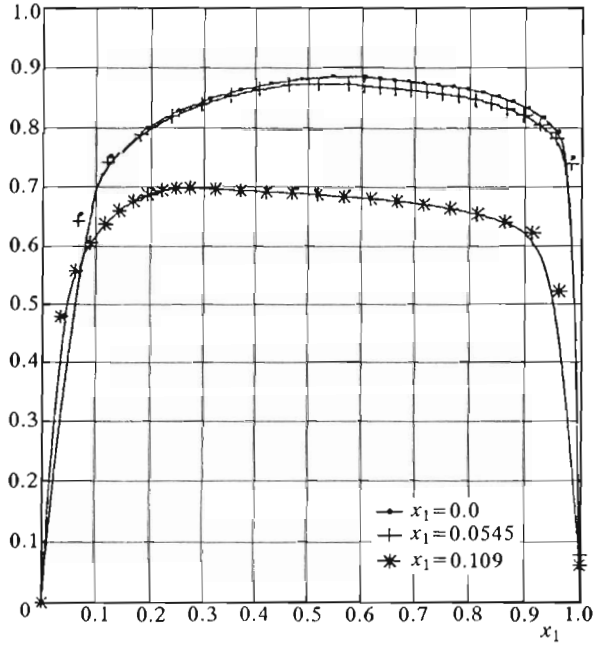


Fig. 8.

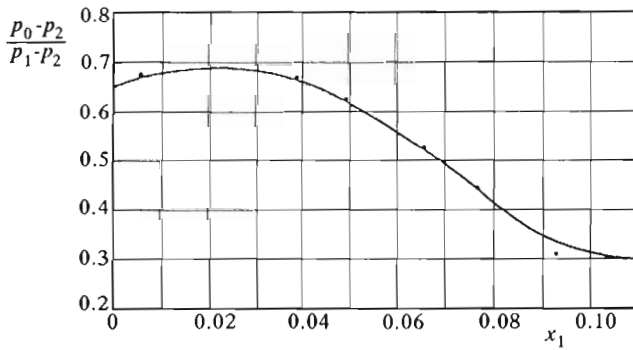


Fig. 9.

It is worth noting that the blockage factor reaches a very high value in the first subdomain as it is shown in Fig.8. Here $x_1 = 0$ is the blockage factor at the root, $x_1 = 0.0545$ is the blockage factor at mid-height and $x_1 = 0.109$ at the tip. From the design point of view the magnitude of so high blockage factor is rather questionable. But one has to take into account that in the presented example the flow is non-dissipative, so it is not realistic. It demonstrates the conditions which have to be fulfilled for the demanded S_1 surfaces on given assumptions and chosen boudary conditions.

The relative pressure drop in the rotor with respect to the pressure drop in the whole stage along meridional streamlines is shown in Fig.9. The degree of reaction is proportional to this factor. It shows the positive, of a rather high value, degree of reaction along the height of the stage.

The surface S_2 for the rotor in the absolute system is shown in Fig.10a and for the relative system in Fig.10b.

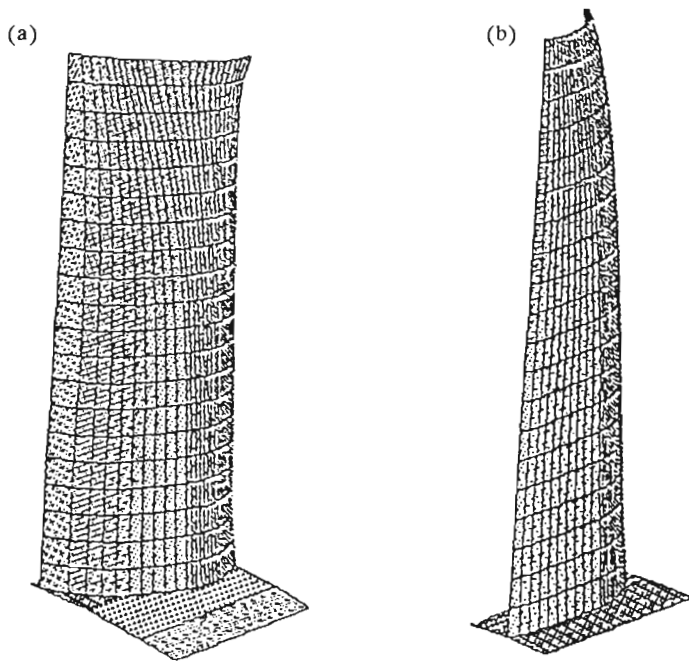


Fig. 10.

7. Conclusions

The paper demonstrates the effectiveness of the algorithm of inverse problem solving for a gas turbine stage shaped by parabolic meridional stream lines (S_1 surfaces).

The boundary conditions for the rotor domain had a specific character which demanded division of this domain into different subdomains. The paper aimed at showing this feature of the problem.

The solution for nondissipative flow has been obtained, but the main idea of the algorithm can be applied also to a dissipative case.

References

1. WENNSTROM A.J., 1974, *On the Treatment of Body Forces in the Radial Equilibrium Equation of Turbomachinery*, Traupel-Festschrift, Juris-Verlag, Zurich
2. BÜTIKOFER J., HÄNDLER M., WIELAND U., 1989, ABB Low-Pressure Steam Turbines- the Culmination of Selective Development, *ABB Rev.*, 8/9
3. PUZYREWSKI R., NAMIEŚNIK K., 1993, Application of Parabolic-Surface Coordinate System to the Inverse Problem of Fluid-Flow Machinery Stage, *Transactions of the Fluid Flow Machinery Institute Polish Academy of Sciences*, Gdańsk, **95**, 197-204
4. PUZYREWSKI R., NAMIEŚNIK K., 1995, Comparison Between Strictly Conical and Paraboloidal Flow Fields in the Presence of Angular Momentum, *Archiv. Mech.*, **47**, 6, 1073-1088
5. PUZYREWSKI R., POZORSKI J., 1993, Conical Flow Model For Turbine Stages, *Arch. Bud. Masz.*, **XL**, 261-282

Problem odwrotny dla osiowosymetrycznego parabolicznego stopnia turbiny gazowej

Streszczenie

Praca zawiera rozwiązanie problemu odwrotnego dla stopnia turbiny gazowej w ramach osiowosymetrycznego modelu. Kształty osiowosymetrycznych powierzchni prądu założono w formie paraboloid. Przepływ jest ściśliwy oraz izentropowy. Rozwiązanie prowadzi do określenia krzywizn kanałów międzyłopatkowych i rozkładu parametrów w całym obszarze stopnia.